Available online at www.sciencedirect.com
ScienceDirect
Journal of Photochemistry and Photobiology A: Chemistry 185 (2007) 231–238
Journal of Photochemistry and Photobiology A:Chemistry
www.elsevier.com/locate/jphotochem

A multi-receptor fluorescence signaling system exhibiting enhancement selectively in presence of Na(I) and Tl(I) ions

Kalyan K. Sadhu, Bamaprasad Bag, Parimal K. Bharadwaj *

Department of Chemistry, Indian Institute of Technology Kanpur, Kanpur 208016, India

Received 13 April 2006; received in revised form 26 May 2006; accepted 19 June 2006
Available online 25 July 2006

Abstract

A PET fluorescence signaling system $\mathbf{L_1}$ has been synthesized in the 'Receptor1-Spacer-Fluorophore-Spacer-Receptor2' format through attachment of a laterally non-symmetric heteroditopic cryptand and a 4,7,10,13-tetraoxa-1-azacyclopentadecane macrocycle at the 9- and 10-positions of anthracene. The cryptand receptor is derivatized with two 2,4-dinitrobenzene groups to impart structural rigidity. This system exhibits selective fluorescence enhancement in presence of Na(I) and Tl(I) ions simultaneously and mimics the AND logic function. The cryptand receptor also binds a Cu(II) ion outside the cavity and allows $\mathbf{L_1}$ to perform as an INHIBIT chemical logic in presence of H^+ and Cu(II) ions.

Keywords: Fluorescence enhancement; Metal ion specificity; Cryptand; Macrocycle; Logic functions

1. Introduction

Design of chemosensors and chemical logics [1–3] through fluorescence enhancement has led to a number of systems in recent years because fluorescence has become one of the most sensitive analytical tools. Such systems can operate on the photo-induced intramolecular electron transfer (PET) mechanism [4] when built in the format, "fluorophore-spacer-receptor". The modular design characteristic of this format allows one to probe specificity as well as mode of logic operation. Several 'two ionic input-one fluorescence output' systems are known in the literature to emulate the AND logic gate behavior [5] where the inputs have been mostly a combination of proton and alkali/alkaline earth cation. Use of a transition metal ion in these cases can be potentially important due to its redox activity. A cryptand-based receptor is ideal here as once a transition metal ion enters the cavity of the receptor, it is isolated from the surroundings that can nullify most if not all, of the quenching pathways [6]. Following this argument, we reported in a recent communication [7], a multi-receptor fluorescence signaling system exhibiting AND logic operation in presence of a transition and Na(I) ions. We show here that once the cryptand core is derivatized with 2,4-dinitrobenzene groups, it acts as a specific receptor for Tl(I). Selectivity is the prime concern in the design of fluorescence signaling probes for biological as well as environmental aspects. Thallium is extensively used now-a-days in photoelectric cells, electronics and semiconductors, lamps, optical lenses, etc. as well as rodenticide. However, its toxic effect poses severe health hazards [8] and so the development of sensors for Tl(I) demands immediate attention. The fluorescence signaling system $\mathbf{L_1}$ (Fig. 1) described herein, exhibits fluorescence enhancement in simultaneous presence of Na(I) and Tl(I) ions selectively to mimic the AND logic action. The choice of the receptors are based on their binding abilities towards different types of metal ions, i.e. the aza-oxa crown ether has a higher binding affinity towards an alkali/alkaline earth metal ion whereas the cryptand is known for their tendency to form highly stable inclusion complexes with transition metal ions due to the cryptate effect. The rigidification of the cryptand architecture with electron-withdrawing groups allows Tl(I) selectively to enter its cavity while Na(I) preferentially complexed to the macrocyclic receptor, hence in the simultaneous presence of both these ions, the PET operative in $\mathbf{L_1}$ from both the receptor ends gets suppressed resulting in fluorescence enhancement. We had shown earlier [9] that attachment of electron-withdrawing 2,4-dinitrobenzene/4-

* Corresponding author. Tel.: +91 512 2597340.
E-mail address: pkb@iitk.ac.in (P.K. Bharadwaj).

1010-6030/$ – see front matter © 2006 Elsevier B.V. All rights reserved.
doi:10.1016/j.jphotochem.2006.06.014

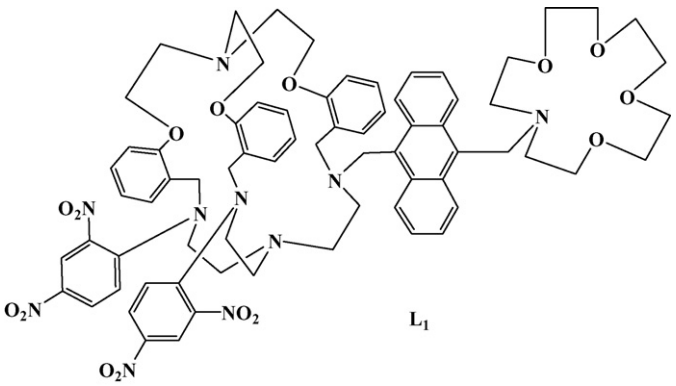

Fig. 1. Chemical structure of $\mathbf{L_1}$.

nitrobenzene groups to the cryptand forces it to bind a Cu(II) ion in MeCN in an exocyclic fashion. Thus, $\mathbf{L_1}$ here exhibits a two input INHIBIT logic action in the simultaneous presence of Cu(II) and H^+.

2. Experimental

2.1. Analysis and measurements

The compounds were characterized by elemental analyses, ^{1}H NMR, ^{13}C NMR and mass (positive ion) spectroscopy. ^{1}H NMR and ^{13}C NMR spectra were recorded on a JEOL JNM-LA400 FT (400 MHz and 100 MHz, respectively) instrument in $CDCl_3$ with Me_4Si as the internal standard. FAB mass (positive ion) data were recorded on a JEOL SX 102/DA-6000 mass spectrometer using argon as the FAB gas at 6 kV and 10 mA with an accelerating voltage of 10 kV and the spectra were recorded at 298 K. Melting points were determined with an electrical melting point apparatus by PERFIT, India and were uncorrected. Elemental analyses were done in an Elementar Vario EL III Carlo Erba 1108 elemental analyzer. UV–visible spectra were recorded on a JASCO V-570 spectrophotometer at 298 K in 10^{-4} to 10^{-5} M concentration. Steady-state fluorescence spectra were obtained with a Perkin-Elmer LS 50B Luminescence Spectrometer at 298 K. Fluorescence quantum yield was determined [10] in each case by comparing the corrected spectrum with that of anthracene ($\phi = 0.297$) [11] in ethanol by taking the area under the total emission. The error in total fluorescence quantum yield (ϕ_{FT}) is 10% for the free ligand, otherwise 5% in each case.

2.2. Materials

All reagent grade chemicals were used as received unless otherwise specified. Triethanolamine, salicylaldehyde, tris(2-aminoethyl)amine, 9-anthracene methanol, 2,4-dinitro-1-chlorobenzene, sodium borohydride and the metal salts were obtained from Aldrich (U.S.A.). Thallium(I) triflate salt was prepared according to the procedure reported in literature. Sodium hydroxide, anhydrous sodium sulfate, potassium carbonate, perchloric acid and thionyl chloride were received from S.D. Fine Chemicals (India). Thionyl chloride and the solvents were freshly distilled prior to use following the literature procedures [12]. The purified solvents were found to be free from impurities, moisture and were transparent in the region of interest. The reactions were carried out under N_2 atmosphere. Chromatographic separation was achieved using 100–200 mesh silica gel obtained from Acme Synthetic Chemicals, India.

2.3. Synthesis

The synthetic route to $\mathbf{L_1}$ is given in Scheme 1.

2.3.1. Synthesis of triethylene glycol ditoluenesulfonate, *1*

Synthesis of this compound was achieved following a literature procedure [13]. Yield: 90%; M. pt. 81 °C (lit. 80.5–81.5 °C); ^{1}H NMR (400 MHz, $CDCl_3$, 25 °C, TMS) δ: 2.39 (s, 6H), 3.54 (t, 12H), 3.75 (t, 4H), 7.40 (d, 4H), 7.82 (d, 4H); ^{13}C NMR (100 MHz, $CDCl_3$, 25 °C, TMS) δ: 144.2, 131.5, 130.9, 128.7, 71.2, 70.0, 62.5, 21.6; ESI-MS, *m/z* (%): 458 (100) [M^+] Anal. calcd. for $C_{20}H_{26}O_8S_2$: C, 52.39; H, 5.72. Found: C, 52.31; H, 5.79%.

2.3.2. Synthesis of 4,7,10,13-tetraoxa-1-azacyclopentadecane, *2*

The macrocycle **2** was synthesized via condensation of **1** with bis-(hydroxyethyl) amine as per the reported [14] procedure. Yield: 35%, M. pt. 29 °C (lit. 34 °C); ^{1}H NMR (400 MHz, $CDCl_3$, 25 °C, TMS) δ: 2.74 (t, $J = 6$ Hz, 4H, NCH_2), 3.03 (s, 1H, NH), 3.55–3.75 (m, 16H, 8× OCH_2); ESI-MS, *m/z* (%): 220 (100) $[M + 1]^+$; Anal. calcd. for $C_{10}H_{21}N_1O_4$: C, 54.78; H, 9.65; N, 6.39. Found: C, 54.69; H, 9.71; N 6.32%.

2.3.3. Synthesis of 1-(9′-methylanthracenyl)-4,7,10,13-tetraoxa-1-azacyclopentadecane, *3*

To a solution of the macrocycle **2** (1.0 g; 4.6 mmol) in dry acetonitrile, anhydrous K_2CO_3 (0.63 g; 4.6 mmol) was added and stirred for 15 min. Solid 9-bromomethyl anthracene (1.25 g, 4.6 mmol) was then added along with a crystal of KI and the reaction mixture was stirred first at 60 °C under nitrogen atmosphere for 12 h and then refluxed for 36 h whereupon a small amount of a yellow solid precipitated out. After cooling to RT, the solvent was removed under vacuum. The solid remained was washed several times with water, extracted with $CHCl_3$ and the organic layer after drying over anhydrous Na_2SO_4, evaporated to dryness to obtain a yellow solid. The product was purified and isolated by column chromatography through a silica gel (100–200 mesh) using 5% ethyl acetate in chloroform as the eluent.

Yield: 68%; ^{1}H NMR (400 MHz, $CDCl_3$, 25 °C, TMS) δ: 2.93 (t, $J = 5.56$ Hz, 4H, 2× NCH_2), 3.48–3.56 (m, 16H, 8× OCH_2) 4.63 (s, 2H, An-CH_2), 7.36 (t, 2H, $J = 7.55$ Hz, An-$H_{3,6}$), 7.44 (t, 2H, $J = 7.55$ Hz, An-$H_{2,7}$), 7.89 (d, $J = 7.79$ Hz, 2H, An-$H_{4,5}$), 8.31 (s, 1H, An-H_{10}), 8.39 (d, 2H, $J = 8.75$ Hz, An-$H_{1,8}$); ^{13}C NMR (100 MHz, $CDCl_3$, 25 °C, TMS) δ: 131.2, 128.9, 127.9, 126.0, 124.8, 71.4, 71.0, 70.4, 70.1, 69.5, 68.7, 60.9, 54.6, 49.8, 45.5, 27.3; FAB-MS, *m/z* (%): 410 (100) $[M + 1]^+$; Anal. calcd.

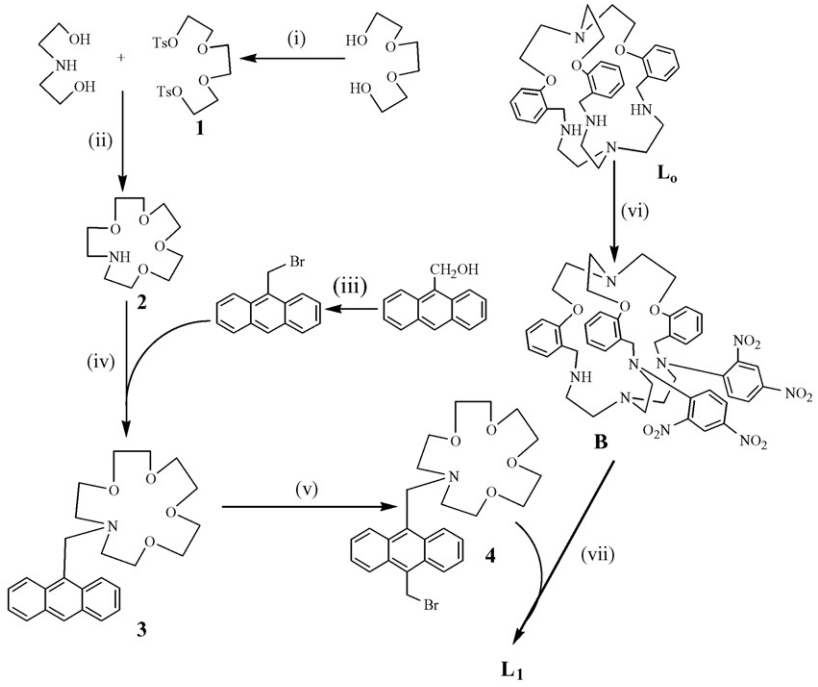

Scheme 1. Synthetic route to $\mathbf{L_1}$. Reagent and conditions: (i) NaOH, *p*-toluene sulfonyl chloride, THF: H_2O (2:1), 0 °C; (ii) Na in *tert*-butanol, 40 °C; (iii) PPh_3, Br_2, MeCN, 25 °C; (iv) K_2CO_3, MeCN, KI; (v) paraformaldehyde, 30% HBr in AcOH, 45 °C, 2 h; (vi) 2,4-dinitro-1-chlorobenzene (1.8 equiv.), K_2CO_3, EtOH, 24 h; (vii) MeCN, K_2CO_3, KI, reflux, 72 h.

for $C_{25}H_{31}N_1O_4$: C, 73.32; H, 7.63; N, 3.42. Found: C, 73.21; H, 7.68; N 3.34%.

2.3.4. Synthesis of 9′-methyl(4,7,10,13-tetraoxa-1-azacyclopentadecanyl)-10′-bromomethyl anthracene, *4*

To a stirring solution of paraformaldehyde (0.190 g; 6.4 mmol) in 30% HBr in AcOH solution (30 mL), compound **3** (2.6 g; 6.4 mmol) was added and heated for 2 h at 40 °C under N_2 atmosphere. The reaction mixture was then poured into ice-water (150 mL) and extracted with $CHCl_3$ (50 mL). The organic layer, after drying over anhydrous Na_2SO_4, was evaporated to dryness under reduced pressure to obtain a deep yellow solid. Recrystallization from acetonitrile yields a yellow solid as the desired product. Yield: 52%; ^{1}H NMR (400 MHz, $CDCl_3$, 25 °C, TMS) δ: 2.45 (t, J = 5.56 Hz, 2× NCH_2, 4H), 3.41–3.54 (m, 16H, 8× OCH_2), 4.13 (s, 2H, An-9-CH_2), 5.09 (s, 2H, An-10-CH_2), 7.41 (t, J = 6.31 Hz, 2H, An-$H_{2,7}$), 7.47 (t, J = 6.83 Hz, 2H, An-$H_{3,6}$), 7.81 (d, J = 8.39 Hz, 2H, An-$H_{4,5}$), 7.99 (d, J = 8.55 Hz, 2H, An-$H_{1,8}$); ^{13}C NMR (100 MHz, $CDCl_3$, 25 °C, TMS) δ: 135.9, 132.3, 129.2, 127.3, 126.3, 125.5, 125.4, 70.2, 69.8, 68.7, 55.4, 52.3, 33.4; FAB-MS, *m/z* (%): 503 (80) [**4**]$^+$; Anal. calcd. for $C_{26}H_{32}N_1O_4$ Br: C, 62.15; H, 6.42; N, 2.79. Found: C, 62.01; H, 6.53; N 2.71%.

2.3.5. Synthesis of the cryptand $\mathbf{L_o}$

Cryptand $\mathbf{L_o}$ was synthesized as reported [15] earlier.

2.3.6. Synthesis of *B*

Cryptand $\mathbf{L_o}$ was allowed to react with 2,4-dinitro-1-chlorobenzene in 1:1.8 molar ratio that afforded tris-, bis- and mono-2,4-dinitrobenzene substituted products. The three components were separated in a silica gel column (100–200 mesh) [16]. The desired product **B** was isolated as a fine yellow crystalline solid. Yield: 0.26 g (29%); M. pt.: 105 °C; ^{1}H NMR (400 MHz, $CDCl_3$, TMS, 25 °C) δ: 2.52 (br s, 6H), 2.70 (br s, 2H), 3.15–3.18 (m, 4H), 3.28–3.36 (m, 6H), 3.93 (s, 2H), 4.13 (br s, 4H), 4.29 (br s, 2H), 4.45 (s, 4H), 6.78–7.18 (m, 14H), 7.93 (d, J = 9.3 Hz, 2H), 8.54 (s, 2H); FAB-MS, *m/z* (%): 892 (100) [**B**]$^+$; Anal. calcd. for $C_{45}H_{49}N_9O_{11}$: C, 60.59; H, 5.54; N, 14.13%. Found: C, 60.63; H, 5.63; N, 14.09%.

2.3.7. Synthesis of $\mathbf{L_1}$

To a solution of **B** (0.45 g; 0.5 mmol) in dry MeCN, anhydrous K_2CO_3 (0.08 g; 0.6 mmol) was added and stirred for 15 min under N_2 atmosphere. Compound **4** (0.25 g; 0.5 mmol) was added to it along with a crystal of KI and the reaction mixture was allowed to reflux for 72 h when a bright yellow solid precipitated out. After cooling to RT, the precipitate was collected by filtration, washed several times with water and extracted with $CHCl_3$. The organic layer after drying over anhydrous Na_2SO_4, was evaporated to dryness to obtain a yellow solid. Purification of the product as a bright yellow powder was done by column chromatography with silica gel (100–200 mesh) and 1% ethyl acetate in chloroform as the eluent. Yield: 79%. ^{1}H NMR (400 MHz, $CDCl_3$, 25 °C, TMS) δ: 2.15 (br s, 6H, 3× CH_2), 2.30 (br s, 6H, 3× CH_2), 2.75 (t, 6H, 3× CH_2), 3.25 (s, 4H, 2× N-$CH_{2(mac)}$), 3.5–3.7 (br s, 22H, 8× $OCH_{2(mac)}$) and 3× N-CH_2-$Ph_{(cryp)}$), 4.25 (br s, 6H, 3× CH_2), 4.48 (s, 2H, An-CH_2-N_{mac}), 4.52 (s, 2H, An-CH_2-N_{cryp}), 7.09 (d, 3H, Ph-H_2), 7.28 (d, 2H, nitroBz-H_6), 7.34 (d, 2H, nitroBz-H_5), 7.43 (d, 3H, Ph-H_5),

7.54 (m, 4H, An-$H_{2,3,6,7}$), 7.68 (t, 6H, Ph-$H_{3,4}$), 8.08 (d, 2H, An-$H_{4,5}$), 8.72 (s, 2H, nitroBz-H_3), 8.99 (d, 2H, An-$H_{1,8}$); ^{13}C NMR (100 MHz, $CDCl_3$, 25 °C, TMS) δ: 156.9, 147.6, 136.6, 131.2, 129.1, 128.2, 127.2, 125.1, 124.7, 123.5, 121.0, 118.0, 110.9, 73.2, 72.6, 71.5, 70.1, 68.9, 66.4, 61.7, 61.0, 54.7, 52.9, 51.8, 49.9, 29.6, 27.4; FAB-MS, *m/z* (%): 1315 (59) $[M+1]^+$; Anal. calcd. for $C_{71}H_{80}N_{10}O_{15}$ [1313.45]: C, 64.93; H, 6.14; N, 18.27. Found: C, 65.07; H, 6.22; N 18.13%.

3. Results and discussion

3.1. UV–visible absorption spectroscopy

The UV–vis absorption properties of **L_1** were determined in different solvents. In all the cases, the absorption spectral pattern of metal-free **L_1** in the 350–450 nm region indicates an overlapping of two different types of transitions: (i) an intramolecular charge transfer (ICT) from the donor N-atom of the cryptand to the acceptor dinitrobenzene groups; (ii) anthracene-localized $\pi \rightarrow \pi^*$ transition and its vibrational structures [17]. However, the vibrational structures are not typical of anthracene due to a possible interaction with the 2,4-dinitrobenzene group in the ground state. The absorption maximum (λ_{max}^{abs}) in the visible region is found to be slightly solvatochromic in nature – it absorbs at 364 nm in non-polar cyclohexane and at 381 nm in a relatively polar DMSO (Table 1). The band at ~260 nm is attributable to the π–π interaction between the phenyl of the side-groups and the anthracene in the ground state along with its $S_0 \rightarrow S_3$ transition, and found to be slightly solvatochromic in nature.

Upon complexation with alkali and alkaline earth metals, the molar extinction coefficient decreases retaining the absorption spectral pattern of **L_1** (Fig. 2a). Complexation with transition as well as heavy metal ions investigated also exhibits similar spectral features except for Cu(II) and Pb(II), where complexation modulates the Frank-Condon vibrational structures of the ligand absorption transitions shifting the absorption maxima towards high energy region. This is indicative of a different binding mode of **L_1** with Cu(II) and Pb(II) in the ground state in contrast to other metal ions. Furthermore, protonation of **L_1** is associated with large increase in molar extinction coefficient (ε) as well as blue shifts of the absorption transitions (Fig. 2b) in the visible region as it enhances the charge transfer character [18] in the molecule. The position of the absorption band in the UV region remains unaffected upon complexation, though the molar extinction coefficient values vary to an extent depending upon the nature of the metal ion.

Table 1
The absorption (λ_{max}^{abs}) and emission (λ_{max}^{LE}), exciplex maxima (λ^{EX}) and fluorescence quantum yield (ϕ_{FT}) of **L_1** in different solvents

Solvents	λ_{max}^{abs}, nm	λ_{max}^{LE}, nm	λ^{EX}, nm	ϕ_{FT}
Cyclohexane	364 (n.d.)	405	523	n.d.
n-Hexane	366 (n.d.)	407	524	n.d.
1,4-Dioxane	373 (18048)	415	525	0.0113
Toluene	378 (10597)	423	522	0.0114
$CHCl_3$	379 (18774)	425	534	0.0043
Ethyl acetate	376 (24159)	419	–	0.0047
THF	379 (27350)	425	544	0.0022
DCM	379 (36002)	424	552	0.0034
DMSO	381 (23406)	428	–	0.0041
Acetone	378 (19292)	422	–	0.0027
DMF	380 (26971)	427	–	0.0039
Ethanol	370 (13442)	420	–	0.0023
Acetonitrile	378 (15411)	422	–	0.0016
Methanol	379 (14778)	419	–	0.0019

3.2. Emission spectral behavior of L_1

The cation free **L_1** exhibits a dual emission consisting of a well-resolved anthracene monomer emission corresponding to locally excited $(LE)^1$ (π–π^*) state along with a red-shifted broad structureless emission centered at 520–570 nm. The operative ICT due to D-π-A fragment of the cryptand moiety is non-emissive [19]. The (0, 0) band of the LE emission is centered at ~402 nm along with the vibrational structures at 425

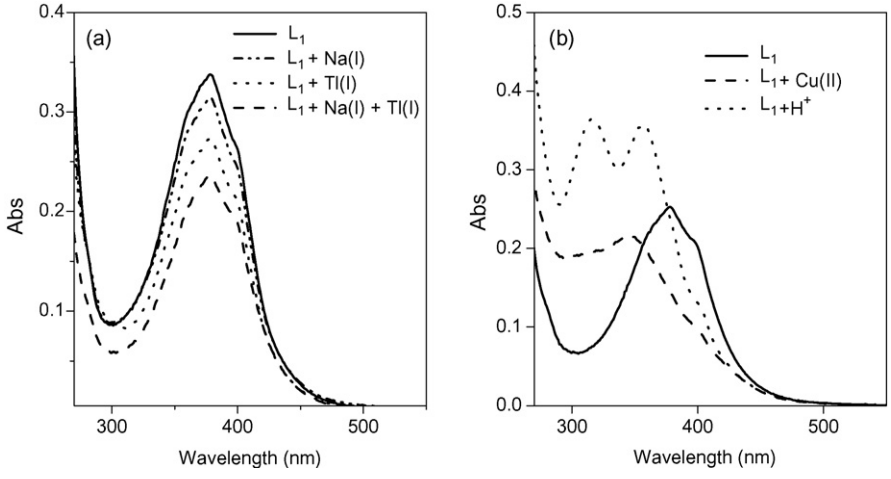

Fig. 2. Absorption spectra of **L_1** in presence of different ionic inputs (a) Na(I), Tl(I), Na(I) + Tl(I) (conc. of **L_1** = 1.2×10^{-5} M) in THF and (b) Cu(II), H^+ (conc. of **L_1** = 1.6×10^{-5} M) in MeCN.

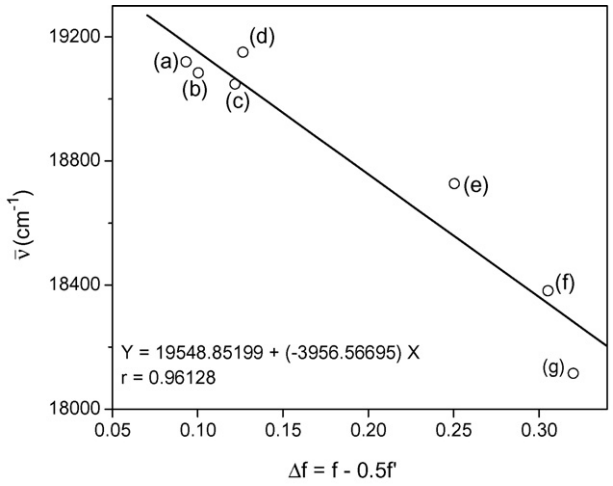

Fig. 3. Plot of ν_{ex} (cm^{-1}) as a function of solvent polarity parameters ($\Delta f = f - 0.5f'$) and its linear regression following Weller's equation. Solvents used (a) *n*-hexane, (b) cyclohexane, (c) 1,4-dioxane, (d) toluene, (e) chloroform, (f) tetrahydrofuran and (g) dichloromethane.

and 441 nm in THF. This emission is found to be slightly solvatochromic in nature, the emission maxima (λ_{max}) is observed at 405 nm in non-polar cyclohexane which is 23 nm blue-shifted in relatively polar DMSO. The absorption and emission maxima and position of exciplex (λ_{ex}) in various solvents are given in Table 1.

The structureless broad emission band ~550 nm is due to an intramolecular exciplex [20] formation which is red-shifted with increase in solvent polarity. A linear relationship is observed when ν_{ex}(max) is plotted (Fig. 3) against solvent polarity parameter in consistent with the Weller's equation [21].

On the basis of the plot, based on the Weller's equation, the excited state dipole moment μ_{ex} for **L$_1$** is calculated to be 31.1 D. The values of μ_{ex} thus obtained should be considered as tentative as it is based on several approximation, the Onsager cavity radius of **L$_1$** in particular. The high value of μ_{ex} in **L$_1$** in comparison to that obtained for intramolecular exciplexes in tris-anthracene substituted **L$_0$** [22] is indicative of a favorable charge transfer in the excited state.

In the absence of any input, the fluorescence quantum yield (ϕ_F) is low due to efficient photo-induced electron transfer (PET) from the HOMO of the donor *tert*-N-atom to the excited fluorophore. However, ϕ_F is found to be higher in solvents with low polarity in comparison to that in the solvents of high polarity. This is because, PET is facilitated in polar media due to favorable charge-dipole and H-bonding interactions with the solvent molecules.

3.3. Fluorescence emission in presence of metal ions

The fluorescence quantum yield of **L$_1$** does not vary to any significant extent in presence of alkali/alkaline earth metal ions. This is because, these ions occupy the macrocyclic receptor (receptor$_1$) only and disrupts the PET process operative from that end where as the cryptand (receptor$_2$) remains empty keeping the PET from that end operational. Even when excess of alkali metal ion is added, the metal may bind to the upper deck of the receptor$_2$ that does not block the PET as observed [22,23] earlier. When both the receptors are simultaneously occupied, only then the PET will be blocked from both ends leading to recovery of fluorescence. However, empirically it is found that only in the simultaneous presence of Na(I) and Tl(I), a 82-fold fluorescence enhancement takes place in MeCN. This shows that derivatization of the cryptand has rendered it to be a Tl(I) specific receptor. The fluorescence spectral behavior of **L$_1$** is shown in Fig. 4a. The shape and peak position of the fluorescence bands do not change upon addition of the metal ions. The fluorescence recovery of **L$_1$** selectively in presence of Tl(I) and Na(I) satisfactorily mimics an AND logic gate function operating with excitation energy as the power supply, metal ions as inputs and the fluorescence as output. A lower fluorescence recovery is observed when K(I) is used in place of Na(I) along with Tl(I) as the tetraoxaazacyclopentadecane macrocycle has a higher affinity [24] towards Na(I) compared to K(I). The fluorescence quan-

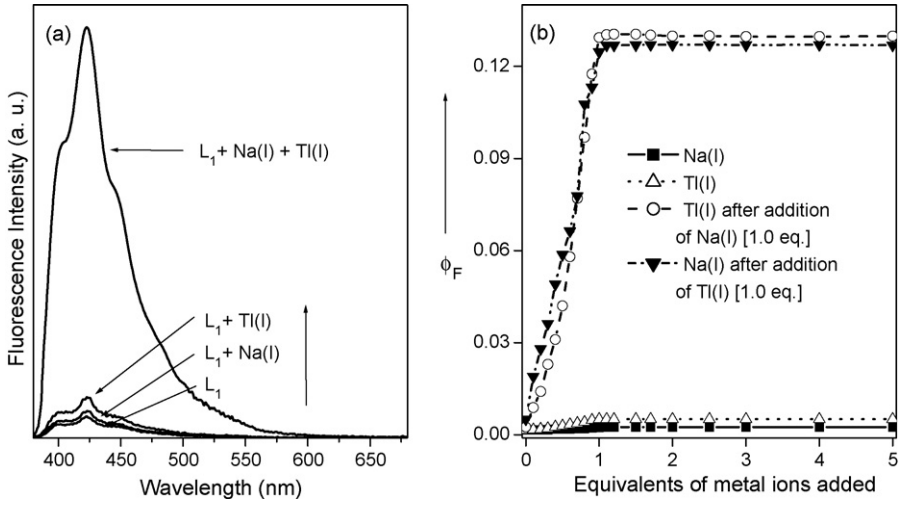

Fig. 4. (a) Fluorescence emission spectra for **L$_1$** with different inputs exhibiting AND logic function in MeCN; (b) plot of fluorescence quantum yield of **L$_1$** (conc. 1.4×10^{-6} M) as a function of equivalents of metal ion added in MeCN.

Table 2
Fluorescence output of $\mathbf{L_1}$ in presence of different ionic inputs in MeCN and THF

Ionic inputs		Fluorescence quantum yield[a] (ϕ_F), (enhancement factor[b]), [output state[c]]	
Input 1 (I_1), [state][d]	Input 2 (I_2), [state][d]	MeCN	THF
– [0]	– [0]	0.0016 (1) [0]	0.0022 (1) [0]
Na(I) [1]	– [0]	0.0025 (2) [0]	0.0021 (1) [0]
K(I) [1]	– [0]	0.0023 (1) [0]	0.0022 (1) [0]
Li (I) [1]	– [0]	0.0016 (1) [0]	0.0020 (1) [0]
– [0]	Mn(II) [1]	0.0018 (1) [0]	0.0021 (1) [0]
– [0]	Fe(II) [1]	0.0022 (1) [0]	0.0020 (1) [0]
– [0]	Co(II) [1]	0.0017 (1) [0]	0.0020 (1) [0]
– [0]	Ni(II) [1]	0.0021 (1) [0]	0.0025 (1) [0]
– [0]	Cu(II) [1]	0.0009 (<1) [0]	0.0019 (1) [0]
– [0]	Zn(II) [1]	0.0022 (1) [0]	0.0028 (1) [0]
– [0]	Tl(I) [1]	0.0051 (3) [0]	0.0049 (2) [0]
– [0]	Pb(II) [1]	0.0021 (1) [0]	0.0026 (1) [0]
– [0]	Ag(I) [1]	0.0019 (1) [0]	0.0036 (2) [0]
H^+ [1]	H^+ [1]	0.0528 (33) [1]	0.0858 (39) [1]
Na(I) [1]	Mn(II) [1]	0.0029 (2) [0]	0.0030 (1) [0]
Na(I) [1]	Fe(II) [1]	0.0027 (2) [0]	0.0026 (1) [0]
Na(I) [1]	Co(II) [1]	0.0023 (1) [0]	0.0031 (1) [0]
Na(I) [1]	Ni(II) [1]	0.0033 (2) [0]	0.0020 (1) [0]
Na(I) [1]	Cu(II) [1]	0.0002 (<1) [0]	0.0024 (1) [0]
Na(I) [1]	Zn(II) [1]	0.0031 (2) [0]	0.0039 (2) [0]
Na(I) [1]	Cd(II) [1]	0.0023 (1) [0]	0.0036 (2) [0]
Na(I) [1]	Pb(II) [1]	0.0039 (2) [0]	0.0024 (1) [0]
Na(I) [1]	Tl(I) [1]	0.1304 (82) [1]	0.1614 (73) [1]
Na(I) [1]	Ag(I) [1]	0.0046 (3) [0]	0.0089 (4) [0]
K(I) [1]	Tl(I) [1]	0.0720 (45) [1]	0.1056 (48) [1]
Mn(II) [1]	Na(I) [1]	0.0022 (1) [0]	0.0027 (1) [0]
Fe(II) [1]	Na(I) [1]	0.0021 (1) [0]	0.0025 (1) [0]
Co(II) [1]	Na(I) [1]	0.0019 (1) [0]	0.0019 (1) [0]
Ni(II) [1]	Na(I) [1]	0.0021 (1) [0]	0.0020 (1) [0]
Cu(II) [1]	Na(I) [1]	0.0004 (<1) [0]	0.0029 (1) [0]
Zn(II) [1]	Na(I) [1]	0.0028 (2) [0]	0.0068 (3) [0]
Tl(I) [1]	Na(I) [1]	0.1271 (79) [1]	0.1685 (77) [1]

[a] Experimental conditions: conc. of free ligand: 1×10^{-6} M; conc. of ionic input: $\sim 1 \times 10^{-5}$ M; $\lambda_{ex} = 378$ nm; excitation and emission band-pass: 5 nm; temperature: 298 K; The error in ϕ_F is within 10%.
[b] FE: fluorescence enhancement in comparison to the cation free ligand.
[c] Fluorescence output state: low [0] and high [1].
[d] Chemical input state: absence [0] and presence [1]; I_1 and I_2 are the first and second ionic inputs, respectively.

tum yields of $\mathbf{L_1}$ with different ionic inputs are collected in Table 2.

Fluorescence titration of $\mathbf{L_1}$ as a function of concentrations of Na(I) and Tl(I) as inputs (Fig. 4b) indicates a 1:1 complex formation with each of the ionic inputs. The final enhancement is found to be almost same when Na(I) is added first followed by Tl(I) or vice versa. A similar nature of the fluorescence titration curve is observed with K(I) and Tl(I) as inputs. The complex stability constants (K_s) are determined from regression plots obtained from the fluorescence intensity changes following a reported procedure [17,25]. The values obtained are found to be consistent with those available in the literature with good correlation coefficients ($\geq$0.99). The K_s is found to be of the order of $\sim 10^6\,M^{-1}$ for Tl(I) in presence of Na(I)/K(I). It is further revealed that the sequence of ionic inputs does not affect the K_s value indicating insignificant inter-receptor interference in the binding of the inputs.

3.4. Fluorescence emission with protons and logic actions with metal ions

In presence of H^+ (1×10^{-3} M) as input, the fluorescence of $\mathbf{L_1}$ enhances ~35-fold in dry or aqueous THF/MeCN medium. Protons engage the lone pair of donor nitrogens of both the receptors causing fluorescence enhancement by effectively blocking the PET. However, hydrated metal perchlorate salts also can generate protons in organic solvents. In order to verify that the fluorescence enhancement is due to the metal ion added and not because of protonation, certain controlled experiments were carried out [22,26]. If the proton generation in the medium by the metal salts were to be responsible for suppression of PET, then the extent of enhancement for all the metal ions investigated should have been almost the same, which is unlikely here.

With protons being one of the inputs to $\mathbf{L_1}$, the extent of fluorescence enhancement of $\mathbf{L_1}$ depends upon the metal ion to be used as the second input. For example, when Na(I) is added followed by H^+, $\mathbf{L_1}$ exhibits a ~50-fold enhancement in THF as Na(I) is selectively bound in the macrocycle (receptor$_1$). On the other hand, addition of Tl(I) followed by H^+, a ~65-fold enhancement is observed in THF. A truth table based on these ionic inputs along with the fluorescence quantum yields as the output is given below (Table 3).

From our earlier experiments [9], it is known that when the core of a cryptand receptor is selectively derivatized with 2,4-dinitrobenzene groups, it exhibits fluorescence enhancement in MeCN selectively in presence of Cu(II), the metal favoring exocyclic coordination to cryptand. Compound $\mathbf{L_1}$ does not exhibit any enhancement in the simultaneous presence of Na(I) and Cu(II) ions. Instead, further quenching ($\phi_F = 0.0002$, MeCN) is observed. Although, Cu(II) binds the cryptand from outside (as supported by the absorption spectra that exhibits a different binding mode for $\mathbf{L_1}$ with Cu(II) ion in comparison to other metal ions) and suppresses the PET operative at that end, a possible metal–fluorophore (M–F) interaction in $\mathbf{L_1}$ due to steric constraints lead to quenching of fluorescence again. The fluorescence spectra of $\mathbf{L_1}$ shows an exciplex at 552 nm upon Cu(II) binding, a characteristics that was previously observed [9] with cryptand based receptors when derivatized with electron withdrawing side arms. However, with H^+ and Cu(II) being the inputs, $\mathbf{L_1}$ exhibits a two input INHIBIT logic action. In MeCN, fluorescence of $\mathbf{L_1}$ is quenched due to PET operative; in presence of Cu(II), the fluorescence is still low ('0' state). In the presence of H^+, $\mathbf{L_1}$ exhibits a 33-fold fluorescence enhancement ($\phi_F = 0.0528$ in MeCN, '1' state). But in the simultaneous presence of both H^+ and Cu(II), the fluorescence is quenched ($\phi_F = 0.0039$ in MeCN, '0' state). The fluorescence spectral pattern in presence Cu(II) and H^+ inputs and the corresponding truth table with logic circuit for INHIBIT function are given in Fig. 5.

Table 3
Fluorescence quantum yield of $\mathbf{L_1}$ in presence of H^+ and Na(I) or Tl(I) in THF

Inputs		Output, ϕ_F, FE[b], [state][c]	Inputs		Output, ϕ_F, FE[b], [state][c]
I_1 [state][a]	I_2 [state][a]		I_1 [state][a]	I_2 [state][a]	
None [0]	None [0]	0.0022, 1, [0]	None [0]	None [0]	0.0022, 1, [0]
Na(I) [1]	None [0]	0.0021, 1, [0]	Tl(I) [1]	None [0]	0.0035, 2, [0]
None [0]	H^+ [1]	0.0858, 39, [1]	None [0]	H^+ [1]	0.0858, 39, [1]
Na(I) [1]	H^+ [1]	0.1114[d], 51, [1]	Tl(I) [1]	H^+ [1]	0.1408[e], 64, [1]

[a] Chemical input state: absence [0] and presence [1]; I_1 and I_2 are the first and second ionic inputs, respectively.
[b] FE: fluorescence enhancement in comparison to the cation free ligand.
[c] Fluorescence output state: low [0] and high [1].
[d] $\phi_F = 0.074$ in MeCN (46-fold FE).
[e] $\phi_F = 0.089$ in MeCN (56-fold FE) in comparison to that of $\mathbf{L_1}$ in MeCN.

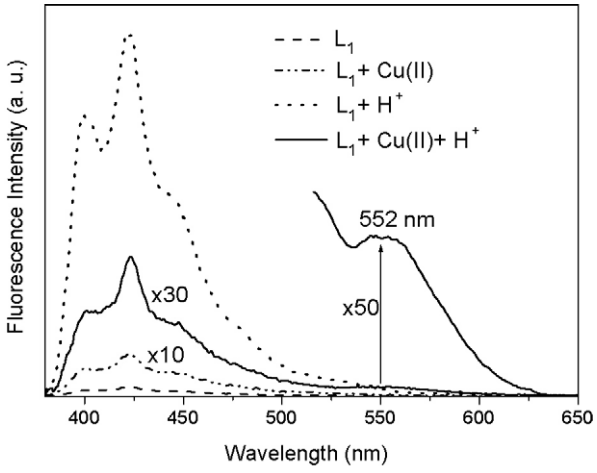

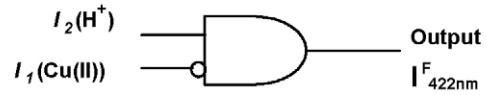

Inputs		Output
I_1 [state]	I_2 [state] ϕ_{FT}, FE, [state]	
none [0]	none [0]	0.0016, 1, [0]
Cu(II) [1]	none [0]	0.0009, 1, [0]
none [0]	H^+ [1]	0.0528,33, [1]
Cu(II) [1]	H^+ [1]	0.0039,2, [0]

Fig. 5. Fluorescence spectral behavior of $\mathbf{L_1}$ (conc. 1.5×10^{-6} M) alone and in presence of Cu(II) and H^+ in MeCN. Corresponding truth table with fluorescence quantum yield output and the logic circuit of INHIBIT gate.

4. Conclusion

In conclusion, The PET signaling system $\mathbf{L_1}$ has been shown to operate either as a molecular AND or INHIBIT logic gate depending upon the nature of the pair of ionic inputs. It acts as an AND logic gate specifically in presence of Na(I) and Tl(I) ions. Structural rigidity imposed through attachment of 2,4-dinitrobenzene groups to the cryptand results in selective Tl(I) inclusion, leaving the counter anion (OTf^-) outside the cavity of the cryptand. Tl(I) selective fluorescence signaling is rare in literature. On the other hand, in the simultaneous presence of Cu(II) and H^+ as the inputs, $\mathbf{L_1}$ performs as an INHIBIT logic gate.

Acknowledgements

Financial support for this work from the Department of Science and Technology, New Delhi, India is gratefully acknowledged. K.K.S. thanks CSIR, New Delhi, India for a Junior Research Fellowship.

Appendix A. Supplementary data

Supplementary data associated with this article can be found, in the online version, at doi:10.1016/j.jphotochem.2006.06.014.

References

[1] A.P. de Silva, N.D. McClenaghan, C.P. McCoy, in: V. Balzani (Ed.), Electron Transfer in Chemistry, vol. 5, Wiley–VCH, Weinheim, 2001.
[2] (a) V. Balzani, M. Venturi, A. Credi (Eds.), Molecular Devices and Machines, A. Journey into the Nano World, Wiley–VCH, Weinheim, 2003; (b) M.D. Ward, J. Chem. Educ. 78 (2001) 321.
[3] (a) A.P. de Silva, N.D. McClenaghan, Chem.-Eur. J. 10 (2004) 574; (b) G.J. Brown, A.P. de Silva, S. Pagliari, Chem. Commun. (2002) 2461; (c) F.M. Raymo, Adv. Mater. 14 (2002) 401.
[4] (a) G.J. Kavarnos, Fundamentals of Photoinduced Electron Transfer, VCH, Weinheim, 1993; (b) A.W. Czarnik, J.-P. Desvergne (Eds.), Chemosensors for Ion and Molecule Recognition, Kluwer, Dordrecht, 1997.
[5] (a) S. Uchiyama, G.D. McClean, K. Iwai, A.P. de Silva, J. Am. Chem. Soc. 127 (2005) 8920; (b) J.F. Callan, A.P. de Silva, N.D. McClenaghan, Chem. Commun. (2004) 2048; (c) A.P. de Silva, G.D. McClean, S. Pagliari, Chem. Commun. (2003) 2010; (d) H.-F. Ji, R. Dabestani, G.M. Brown, J. Am. Chem. Soc. 122 (2000) 9306; (e) A.P. de Silva, H.Q.N. Gunaratne, C.P. McCoy, J. Am. Chem. Soc. 119 (1997) 7891; (f) A.P. de Silva, H.Q.N. Gunaratne, C.P. McCoy, Nature 364 (1993) 42.
[6] (a) J.A. Kemlo, T.M. Shepard, Chem. Phys. Lett. 47 (1977) 158; (b) A.W. Varnes, R.B. Dodson, E.L. Wehry, J. Am. Chem. Soc. 94 (1972) 946.
[7] B. Bag, P.K. Bharadwaj, Chem. Commun. (2005) 513.
[8] (a) S. Galvan-Arzate, A. Santamaria, Toxicol. Lett. 99 (1998) 1; (b) J.O. Nriagu (Ed.), Thallium in the Environment, Wiley Series in Advances in Environmental Science and Technology, Wiley–Interscience, 1998.

[9] (a) B. Bag, P. Mukhopadhyay, P.K. Bharadwaj, J. Photochem. Photobiol. A 181 (2006) 215;
(b) B. Bag, P.K. Bharadwaj, Org. Lett. 7 (2005) 1573.
[10] (a) S. Uchiyama, Y. Matsumura, A.P. de Silva, K. Iwai, Anal. Chem. 75 (2003) 5926;
(b) M. Onoda, S. Uchiyama, T. Santa, K. Imai, Anal. Chem. 74 (2002) 4089.
[11] J.B. Birks, Photophysics of Aromatic Molecules, Wiley–Interscience, New York, 1970.
[12] W.L.F. Armarego, D.D. Perrin, Purification of Laboratory Chemicals, 3rd ed., Pergamon Press, Oxford, UK, 1988.
[13] M. Ouchi, Y. Inoue, Y. Liu, S. Nagamune, S. Nakamura, K. Wada, T. Hakushi, Bull. Chem. Soc. Jpn. 63 (1990) 1260.
[14] D. Parker (Ed.), Macrocycle Synthesis: A Practical Approach, Oxford University Press, 1996.
[15] K.G. Ragunathan, P.K. Bharadwaj, Tetrahedron Lett. 33 (1992) 7581.
[16] P. Mukhopadhyay, P.K. Bharadwaj, A. Krishnan, P.K. Das, J. Mater. Chem. 12 (2002) 2786.
[17] B. Bag, P.K. Bharadwaj, J. Phys. Chem. B 109 (2005) 4377.
[18] A. Horvath, K.L. Stevenson, Charge-transfer Photochemistry of Coordination Compounds, VCH, Weinheim, Germany, 1993.
[19] P. Mukhopadhyay, B. Sarkar, P.K. Bharadwaj, K. Nättinen, K. Rissanen, Inorg. Chem. 42 (2003) 4955.
[20] M. Gordon, W.R. Ware (Eds.), The Exciplex, Academic Press Inc., New York, 1975.
[21] Weller's equation: $\nu_{ex} = \nu_{ex}(0) - (2\mu_{ex}^2/hca^3)(f - 0.5f')$ where ν_{ex} (cm^{-1}) is the fluorescence maximum of exciplex emission in a given solvent, $\nu_{ex}(0)$ is that in vacuum, μ_{ex} is the dipole moment of the exciplex, a is the Onsager cavity radius, $(f - 0.5f')$ is the solvent polarity parameter measured from its dielectric constant (ε) and refractive index (η) [$f = (\varepsilon - 1)/2\varepsilon + 1)$ and $f' = (\eta^2 - 1)/(2\eta^2 + 1)$]. The Onsager cavity radius along with the first solvation shell for L_1 is approximated to ~13 Å. For solvent polarity parameters, please refer H. Beens, A. Weller, Chem. Phys. Lett. 2 (1968) 82.
[22] P. Ghosh, P.K. Bharadwaj, J. Roy, S. Ghosh, J. Am. Chem. Soc. 119 (1997) 11903.
[23] P.K. Bharadwaj, Prog. Inorg. Chem. 51 (2003) 251.
[24] R.M. Izatt, K. Pawlak, J.S. Bradshaw, R.L. Bruening, Chem. Rev. 91 (1991) 1721.
[25] S. Fery-Forgues, M.-T. Le Bries, J.-P. Guetté, B. Valeur, J. Phys. Chem. 92 (1988) 6233.
[26] B. Ramachandran, G. Saroja, N.B. Sankaran, A. Samanta, J. Phys. Chem. B 104 (2000) 11824.